3D Electrohydrodynamic Printing of Contact Lens-like Chloramphenicol-loaded Patches for Corneal Abrasions Treatment

3D Electrohydrodynamic Printing of Contact Lens-like Chloramphenicol-loaded Patches for Corneal Abrasions Treatment

Renyuan Sun [a,b,c], Baolin Wang [a,b,c,*], Xinyue Li [d], Ming-Wei Chang [e], Xinghao Yan [a,b,c], Longfei Zhang [a,b,c]

[a] *State Key Laboratory of Reliability and Intelligence of Electrical Equipment, Hebei University of Technology, 300401 Tianjin, China*

[b] *Tianjin Key Laboratory of Bio-electromagnetic and Neural engineering, Hebei University of Technology, 300132 Tianjin, China*

[c] *Hebei Key Laboratory of Bioelectromagnetics and Neuroengineering, School of Health Sciences and Biomedical Engineering, Hebei University of Technology, 300132 Tianjin, China*

[d] *School of Electrical Engineering, Hebei University of Technology, Tianjin 300401, China*

[e] *Nanotechnology and Integrated Bioengineering Centre, Jordanstown Campus, University of Ulster, Newtownabbey BT37 0QB, UK*

ABSTRACT

Corneal abrasion is a common traumatic emergency, which can cause eyelid photophobia, tearing, and obvious foreign body sensation and pain. In this study, the 3D contact lens-like chloramphenicol-loaded patches composed of well-organized micron fibers was prepared via electrohydrodynamic (EHD) printing to treat corneal abrasions. The main material of these patches was cellulose acetate (CA), and chloramphenicol (CAM) was loaded in the patches. EHD printing could realize the micron fibers stacked layer by layer to form a customizable shape suitable for eye wear. Herein, the surface morphology, chemical as well as physical properties, transparency, drug release behaviors and biocompatibility of the patches loading various concentrations of CAM were studied. It was found that the CAM-loaded patches had the 3D hemispherical shape similar to contact lens and smooth surface morphology. Moreover, patches loaded with different concentrations of CAM all maintained good

water absorption, hydrophilicity, light transmittance, and biocompatibility. The drug release curves of CAM-loaded patches showed that the contact lens-like patches had high loading efficiency and could achieved sustained release of CAM, indicating the clinical potential in the treatment of corneal abrasions.

Keywords: Patches, Contact lens-like, Corneal abrasions, EHD printing, Cellulose acetate

1. Introduction

The corneal is the outermost layer of the eye, which makes it more susceptible to injury. Nearly 13% of emergency department visits involve ophthalmological diagnosis; among them, corneal abrasions account for nearly 45%[1]. Eye drops are the traditional treatment of corneal abrasions[2]. However, the high frequency of eye drops to reach the therapeutic concentration is inconvenient, costly, making patients uncomfortable and causing toxic even adverse reactions in the eye or the whole body[3-5]. To overcome these limitations, novel delivery systems and devices for treating corneal abrasions have been explored[6, 7]. It has been reported that soaking contact lenses in the drug solutions could realize controlled and sustained drug delivery[8, 9], which is more efficient than eye drops, and has larger fractional uptake and higher bioavailability[3, 5, 10]. However, most of the drugs only exist on the surface of the contact lens, leading to the delivery of drugs lasting only several hours[11, 12], which is far from clinical requirement.

Fibers with sub-micron scale are excellent candidates for drug delivery with specific benefits relating to surface area, uniformity, porosity, mechanical strength and more efficient dosage forming[13]. Sub-micron fibers could deliver the drug to the site of action at a controllable rate to achieve sustainable release of the drug[14]. Electrospinning is a simple and highly versatile technique that can be used for mass fabrication of continuous sub-micron fibers from various polymers and composites[15]. The mechanism involves ejection of an ultrafine jet from an electrically charged polymer solution at the critical value and elongated droplet solidifies into sub-micron

filaments[16]. However, the deposition of the fibers is random produced by electrospinning and this usually limits its use for preparing well-ordered architectures[17]. Baker et al produced coaxial nanofibers loading moxifloxacin hydrochloride and pirfenidone to realize antibiotic and anti-scarring[18]. But the possibility of wearing and improving the comfort of patients were not considered. To applied in ocular region for treating corneal abrasions, the comforts of the patients could be significantly improved if the treating system can be worn in the eyes and had no effect on the eyesight. For this purpose, the shape of the treating system is especially important.

Electrohydrodynamic (EHD) printing is conducted in similar principles to electrospinning. The working distance between nozzle and conductive collector is short in EHD printing and the continuously jets could be digitally controlled deposition based on materials to create ordered geometry, which is different from the random structure obtained via electrospinning[19]. Thus, EHD printing could fabricate customize drug-loaded sub-micron fibers composites which satisfied the shape of eyeball for treating corneal abrasions with high loading efficiency and comforts. Besides, transmission of light is another key factor for drug loaded system to cure the patient suffering from eye disease. According to our previous work, cellulose acetate (CA) fibers composites showed great light transmission[20]. Besides, CA is biocompatible, biodegradable, nonirritating, and nontoxic[21]. Due to its excellent mechanical properties and affinity, this polymer has been extensively studied and used in wound dressings, and drug carrier to achieve effective wound healing[22]. In addition, there are also researches demonstrating that CA is a promising biological substance for tissue engineering, stem cell research, and regenerative medicine[23].

Chloramphenicol (CAM) is a broad-spectrum antibiotic effective against both Gram-positive and Gram-negative bacteria[24], which is widely used in anti-infection formulations for acute bacterial conjunctivitis local treatment of eye infections in form of eye-drops or ointments[25]. In this study, EHD printing was applied to prepare a CAM-loaded CA patches which were composed of sub-micron fibers and could achieve sustained release of CAM to effectively treat corneal abrasions. The CAM-loaded CA

patches produced by EHD printing had a contact-lens like shape, so that could be customized to be wore in the eye directly. Besides, CA patches had good light transmission, which could treat the corneal abrasions without affecting the eyesight of the patients and improve the comfort of patients. The structures of CA patches were observed by optical microscopy and scanning electron microscopy (SEM). The physical properties of the patches were characterized by Fourier infrared spectroscopy (FTIR), contact angle analysis, and tensile testing. The drug release behaviors of CAM from the CA patches were also investigated. Results clearly indicated that this kind of contact-lens like CAM-loaded CA patches had great potential to be applied in treating corneal abrasions.

2. Material and methods

2.1. Materials

Cellulose acetate (CA, Mn~30000) was purchased from Sigma-Aldrich (America). Chloramphenicol (CAM) and phosphate buffered saline (PBS, PH=7.2~7.4) was purchased from Solarbio (Beijing, China). Acetic acid was supplied by Damao (Tianjin, China). Purified water was supplied by a Millpore Milli-Q Reference ultra-pure water purifier (USA). All materials were used as received without further purification treatment. All chemicals and reagents used were of analytical grade.

2.2. Solution preparation and contact-lens like CAM-loaded CA patches printing

Firstly, CA, CAM and acetic acid was put into a glass bottle and placed on the magnetic stirrer (VELP ARE, Italy). The concentration of CA was 17% of the total solution mass fraction, and the concentration of CAM was set at 0.5%, 1%, 1.5% of the total solution mass fraction, respectively. Besides, the rotation speed of the magnetic stirrer was stable at 300 rpm, and the stirring time was 5 hours to obtain a uniform and transparent mixed solution. The entire process was carried out under ambient temperature (25℃).

The schematic diagram of production process for the contact-lens like CAM-loaded CA patches by EHD printing system is shown in Fig. 1a. The EHD printing platform mainly consisted of three components: a high-voltage supply generating ≈ 30KV (DC,

Dongwen, Tianjin, China), a syringe pump (LSP01-3A, LongerPump, China), and a high-resolution X-Y-Z movement stage (Hongxia automatic control equipment Co., Guanghou, China). CA solutions were loaded into a 5ml syringe, which were controlled by the syringe pump. A stainless 18G nozzle was mounted on the Z-axis and linked to the positive terminal of the high voltage supply. The conductive glass was placed on the grounded X-Y moving stage as the collection substrate. To conduct the EHD process, high voltage was utilized, and the syringe pump was initiated to simultaneously feed CA solutions to the nozzle. The deposition of CA fibers can be effectively controlled to produce contact-lens like structures by changing the movement of X-Y-Z stage according to the specific user design. The speed of X-Y-Z stage was within the range 5 $mm \cdot s^{-1}$. The applied voltage of coaxial nozzle and conductive glass was set at 3 mm. To keep the cone-jet stable during the EHD process, the flow rate of CA solutions was 0.2 $mL \cdot h^{-1}$. To obtain the 3D contact-lens like CA patches, fabrication proceeded with precise designated fiber layers. All experiments were conducted at the ambient temperature (25℃) and relatively humidity (40~60%).

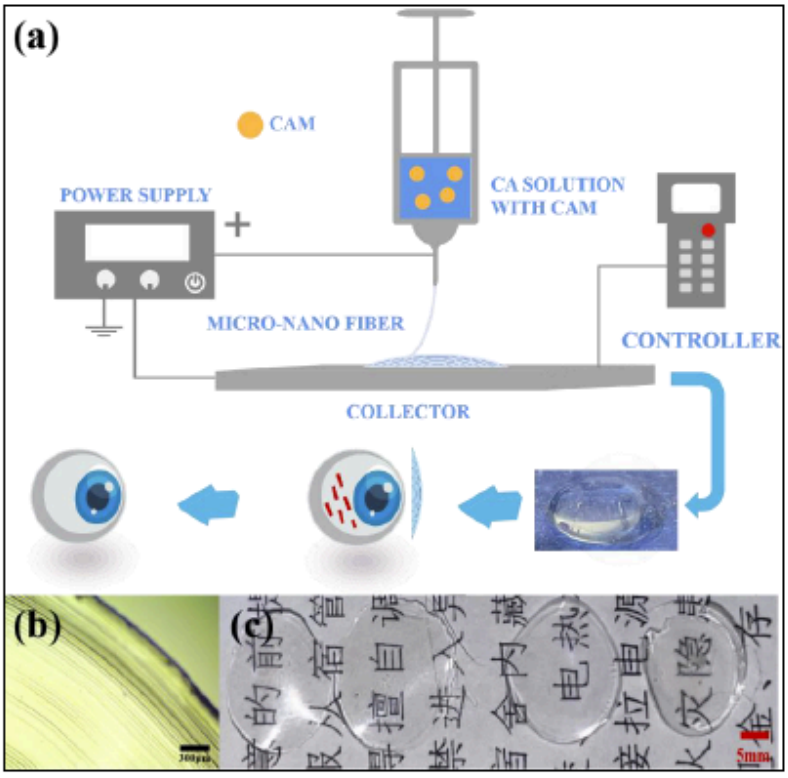

Fig. 1. (a) Schematic diagram of preparation of contact-lens like CAM-loaded CA

patches. (b) The surface photograph of 1% CAM-loaded CA patches. (c)Physical images of CA patches with different concentrations of CAM (from left to right are: CA patches; 0.5% CAM-loaded CA patches; 1% CAM-loaded CA patches; 1.5% CAM-loaded CA patches).

2.3. Characterization of contact-lens like CAM-loaded CA patches

The light transmittance of contact lens-like CA patches loading 0.5%, 1%, and 1.5% CAM and pure CA patches were investigated via a camera in this work. The samples were placed on a printed paper to observe whether the sample influenced visual clarity[26].

Scanning Electron Microscope (SEM, SU8010, HITACHI Corporation, Japan) was used to investigate the surface morphology of contact-lens like CAM-loaded CA patches. All samples were placed on an aluminum stub with double-side tape and were coated with a thin layer of gold for 60s by sputter coating at the current intensity of 10 mA. In this research, the inner structures were imaged by Optical microscopy (OM, Phoenix BMX533-ICCF, China). Topology and roughness of contact-lens like CAM-loaded CA patches were investigated by Atomic Force Microscope (AFM, SPM-9700，Shimadzu Corporation, Japan) with the 10 nm thin tip under the cantilever was used to scan 3×3μm area on the sample surface.

Composition, interactions, and material stability of the contact-lens like CAM-loaded CA patches were investigated by Fourier Transform Infrared (FTIR) spectrophotometer (Bruker Corporation, Zürich, Switzerland). Briefly, 2 mg of the CA patches samples were immersed in 200 mg of potassium bromide (KBr) medium by grinding and compressed into transparent pellets (pressure≈12 MPa for at least 1 min). The scanning spectrums range was 4000~400 cm^{-1}, and the scanning frequency was 16Hz.

XRD analyses were carried out on an X-ray diffractometer (D8 advance, Bruker Corporation, Zürich, Switzerland) to measure the structure information and qualitative analysis of the CA patches samples. All XRD curves were scanned in the range of 10° ~ 50°with a scan speed of $10°\cdot min^{-1}$.

The hydrophilicity of the CA patches is also very important for the corneal abrasions treatment and drug release behaviors[27]. It was investigated by contact angle and interfacial tension analysis (DAS30, KRUSS, Germany) in this study. The sitting drop method was used to study the contact angle of a drop of pure water (5μL) on the surfaces of CA patches loading different concentrations of CAM at the contact point. Each experimental sample was in triplicate.

The swelling degree of contact-lens like CAM-loaded CA patches was also measured at a fixed temperature of 25°C [28]. The samples were weighted using a high precision electronic balance to obtain the (W_d) value. Then, each sample was immersed in PBS solution with a fixed volume of 5 ml. And after 3, 6, 9, and 12 h, the samples were taken out from PBS to be weighted followed by eliminating excess water to obtain the swollen state weight (W). The swelling degree then was computed using the Eq. (1) as follows[29]:

$$Swelling\ degree\ (\%) = \frac{(W-W_d)}{W_d} \times 100\ \% \quad (1)$$

W is the sample's wet weight after immersed in PBS at a fixed volume of 5 mL, while the W_d is the initial dry weight. Each experimental sample was in triplicate.

2.4. In vitro drug-release studies

In this study, drug release behaviors of CAM from contact-lens like CA patches were measured according to a method described in the previous study[30]. The drug loading capacity was calculated according to Eq. (2).

$$L_E\ (\%) = \frac{W_e}{W_m} \times 100 \quad (2)$$

Where L_E represents the drug loading efficiency, W_e is the amount of CAM encapsulated in the CA patches; W_m represents the total weight of the CA patches.

Assays comprised 10 ml release medium (PBS, pH=7.4) with 2.4g of test samples. During whole drug release period, 3 mL of supernatant was extracted for UV detection and replenished with an equal volume of fresh medium at predesigned time intervals. All experiments were carried out in triplicate. The concentration of CAM in supernatant was measured using UV absorption at a wavelength of ~274 nm. The CAM

concentrations in the release medium was calculated through the standard curve.

The proposed drug release mechanism from patches (based on the intrinsic nature of CA) was assumed to be diffusive in nature[31]. To verify this assertion, in vitro drug release data of CAM were fitted to Korsmeyer-Peppas and Higuchi models. The Korsmeyer-Peppas model is normally applied to analyze drug release when the mechanism is not clear. In contrast, the Higuchi model is conventionally used to confirm diffusive drug release from a polymer matrix system. The Korsmeyer-Peppas model is expressed as shown in Eq. (3):

$$\frac{M_t}{M_\infty} = kt^n \tag{3}$$

Here, M_t is the accumulative quantity of drug released at time t, and M_∞ represents the initial drug loading (M_t/M_∞ represents the fraction drug released at time t), k is a constant characteristic and n is the release exponent which indicates the release mechanism[32]. The Higuchi model is presented as shown in Eq. (4):

$$M_t = k_H t^{\frac{1}{2}} \tag{4}$$

Here, M_t is the quantity of cumulative drug release after time t and k_H is the Higuchi constant[33].

2.5. L929 cell culture

To apply contact-lens like CA patches for treating corneal abrasions, the patches should be nontoxic and have good biocompatibility. The biocompatibility of the CA patches was determined using *in-vitro* cell culture assessment. Murine fibroblastic cell lines (L929, Shanghai Zhong Qiao Xin Zhou Biotechnology Co.,Ltd., China) was maintained and cultured in Minimum Essential Medium (MEM, GENOM Biomedical Technology Co., Ltd, China) supplemented with 10% (v/v) fetal bovine serum (FBS, Sijiqing, China), 1% (v/v) penicillin mixed solution (Beijing Solarbio Science & Technology Co., Ltd, China) at 37℃ in a 5% CO_2 atmosphere. Depending on the experiment, cells were seeded in 96-well plates or 6-well plates. The culture medium needed to be changed every 48 h. All samples for cell testing were sterilized under UV light for 24 hours and then fixed in culture medium with sterilized stainless-steel rings.

2.6. CCK-8 cell viability test

100 μL of L929 cell suspension at the density of 1×10^4 cells/mL was placed into a 96-well plate. The proliferation of L929 cells on CA patches loading four different concentrations of CAM was investigated by CCK-8 tests. The Samples were cut into squares (side length=3mm) and then sterilized via UV for 24 hours. Before being added to culture plates, the samples were cut into squares (side length=3mm) and sterilized under UV light for 24 h. After 3 and 5 days of incubation, 10 μL of CCK-8 reagent was added to each well and incubate for an additional 4 h, microplate reader (Nivo, PerkinElmer, USA) was used to measure absorbance at a wavelength of 450 nm.The control group was cells cultured on plain TCP wells, and the blank group was culture medium with CCK-8 solution. The relative cell viability (%) was counted by Eq. (5):

$$Cell\ viability = \frac{Ab.(sample)-Ab.(blank)}{Ab.(control)-Ab.(blank)} \quad (5)$$

Where Ab. represents the absorbance.

2.7. Cell morphology study

Fluorescent microscope (Nikon, Eclipse Ti, Japan) was used to evaluate morphology of L929 cells seeded on CA patches. After fixation with 4% v/v paraformaldehyde for 20 min, L929 cells cultured on CA patches were washed 3 times with PBS (pH = 7.4). Then to increase permeability, cells were permeabilized with 0.1% Triton X-100 in PBS for 5 min and washed by PBS. Subsequently, the cytoskeleton of L929 cells was stained with Alexar Fluor 546 phalloidin (Yeasen Biology Technology Co., Ltd, China) (1:100 dilution) for 20 min, nuclei was stained with 4',6'-diamidino-2-phenylindole hydrochloride (DAPI, Beijing Solarbio Science & Technology Co., Ltd, China) for 5 min. After each staining step, the samples were washed three times with PBS for 5 min each. Finally, L929 cells were observed using an inverted fluorescent microscope. The entire process was carried out under ambient temperature (25℃).

2.8. Cell migration assay

The influence of various concentrations of CAM-loaded CA patches on L929 cell migration was investigated by in vitro scratch assays, L929 cell suspension at the

density of 1×10^5 cells/mL was placed into a 6-well TCP plate, then incubated at 37°C in 5% CO_2 atmosphere until cells aggregated and monolayer formation was evident. A scratch on the cell monolayer surface was made by a 200 μL sterile pipette tip, which was then gently washed with PBS to remove free cells. Fresh culture medium and various patches were added to the scratched specimen well and cells were incubated at 37℃ and 5% CO_2 in an atmosphere. An inverted fluorescent microscope (Nikon, Eclipse Ti, Japan) was respectively used to take images after 0, 24, 48 and 72 h to observe cell migration on the scratched surface.

2.9. Statistical Analysis

Data presented in tables and graphs represent the mean ± standard deviation of at least three independent experiments. Data were analyzed using the ANOVA test, considering $p\leqslant0.05$ as statistically significant.

3. Results and discussion

3.1. Morphology of Contact lens-like drug-loaded film

The CA patches were fabricated according to the scheme illustrated in Fig. 1a. Fig. 1b is the optical microscopy (OM) image of CA patches loaded with 1% CAM. It can be observed that the patches were composed of compact CA fibers and the boundary between fibers could be observed clearly. Besides, the shape of CA patches was circular, and the edge of the patch was an arc. Fig. 1b indicated that the CA patches were fabricated by controllable deposition of CA fibers, the traces of EHD printing can be clearly observed.

Light transmittance is especially important for the dressing treating corneal abrasions due to the reason that it related to the comfort and convenience of patients. Thus, in this study, the light transmittance of the CA patches loading various CAM were investigated. The samples were placed on a printed paper to be observed whether the different concentrations of CAM could influence the visual clarity of the contact lens-like CA patches. As shown in Fig. 1c, compared with others, only the 1.5% CAM-loaded CAM showed the rather inferior light transmittance. However, all the samples demonstrated

good light transmittance and the details could be seen clearly through all the samples. The results indicate the great potential for the patches to be applied in clinical.

SEM images show the morphologies of pure CA patches (Fig. 2a) and 1% CAM-loaded CA patches (Fig. 2b). It could be seen that the patches had smooth surface. Fig.2a1 and 2b1 are the high magnification of Fig.2a and 2b, from which some fibers traces could still be found. However, the traces shown in OM images (Fig.1b) disappeared in low magnification SEM images might be due to fibers fused together within the residual solvent. AFM analysis was carried out to analyze the topology and roughness of the contact lens-like CA patches (Fig. 2c and 2d). The results show a comparison of 3D topology between the contact lens-like pure CA patches and 1% CAM-loaded CA patches. It can be found that the pure CA patches had a rather smoother surface with some humps and the surface roughness (Ra) was 58.19 nm. While the surface roughness of the 1% CAM-loaded CA patches was 62.1 nm, demonstrating that the addition of CAM in the CA patches would increase the surface roughness. The high values of Ra demonstrated that CAM-loaded CA patches could promote the physical adhesion towards the surrounding environment[34].

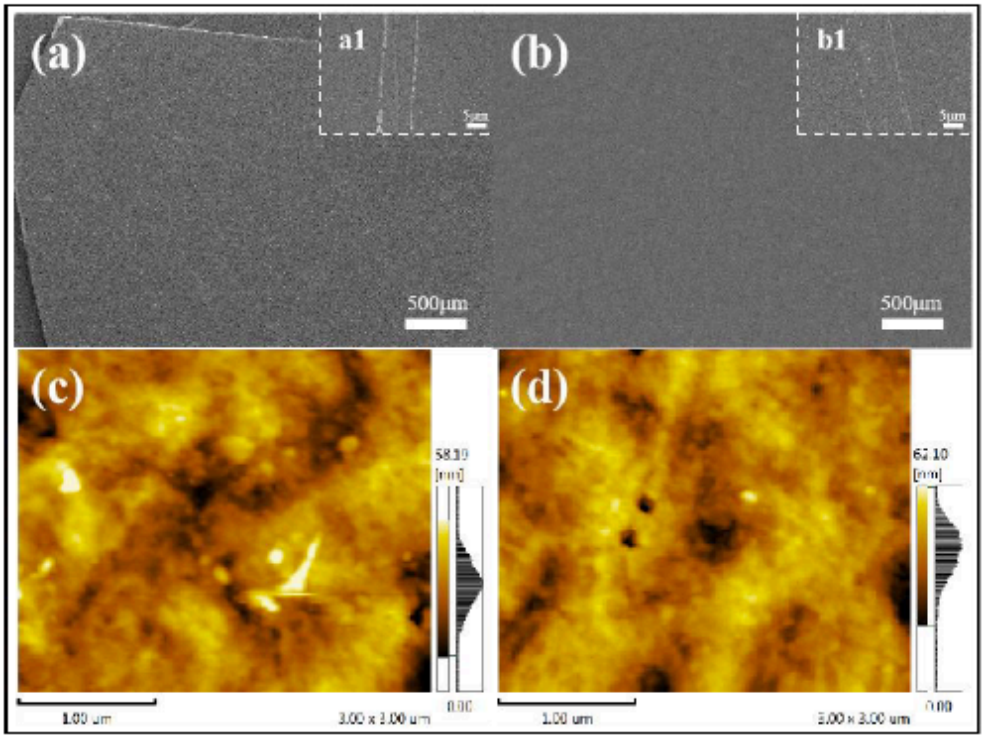

Fig. 2. SEM of CA patches (a) and 1% CAM-loaded CA patches (b). AFM of CA

patches (c) and 1% CAM-loaded CA patches (d).

3.2. FTIR analysis and XRD analysis of contact-lens like CA patches

In addition, previous studies had shown that substance interactions had great effect on drug release patterns[35, 36]. Therefore, the interaction between CA and CAM during EHD printing was explored via XRD patterns and FTIR spectroscopy as shown in Fig. 3. XRD patterns of pure CAM, pure CA and various concentrations of CAM-loaded CA patches are shown in Fig. 3a. CA has a broad absorption peak at 21°, indicating that the crystal structure is amorphous. The diffraction patterns corresponding to CAM indicated it is a crystalline material, as characterized by many sharp diffraction peaks. The crystalline peaks of CAM at 13.1°, 19.03°, 20.8°, and 25.96°mostly appeared, but those peaks were invisible for the fibers prepared using lower CAM content[37]. For the CAM-loaded CA patches, an amorphous halo was observed, suggesting that the CAM was in an amorphous state. The amorphous CAM is conductive to a drug delivery application especially because of the hydrophobicity of CAM[38]. However, the amorphous state in the patches is advantageous for a drug delivery system because it promotes drug release and bioavailability[20]. The amorphous drug results in a higher dissolution rate and thereby may lead to a higher bioavailability for poorly soluble drugs. The FTIR spectrums of contact lens-like CA patches were showed in Fig. 3b. For pure CA powder , the characteristic bands at 3471 cm^{-1}, 1753 cm^{-1}, 1632 cm^{-1}, 1246 cm^{-1} and 1049 cm^{-1} are due to the production of the O-H group, the stretching of C-O group, the stretching of C-O-C group, and the stretching of ether group, respectively[2]. The peak at 3471 cm^{-1} can be clearly observed in the various concentrations of CAM-loaded contact lens-like CA patches. While for pure CAM, the characteristic peaks belongs to the amide or nitro group at 1683 cm^{-1} and 1344 cm^{-1} respectively[39], which could be observed in the CA patches loading various concentrations of CAM. Hence, CAM maintained the stability in the contact lens-like drug-loaded CA patches during the EHD printing, and there were no physical incompatibilities between the components.

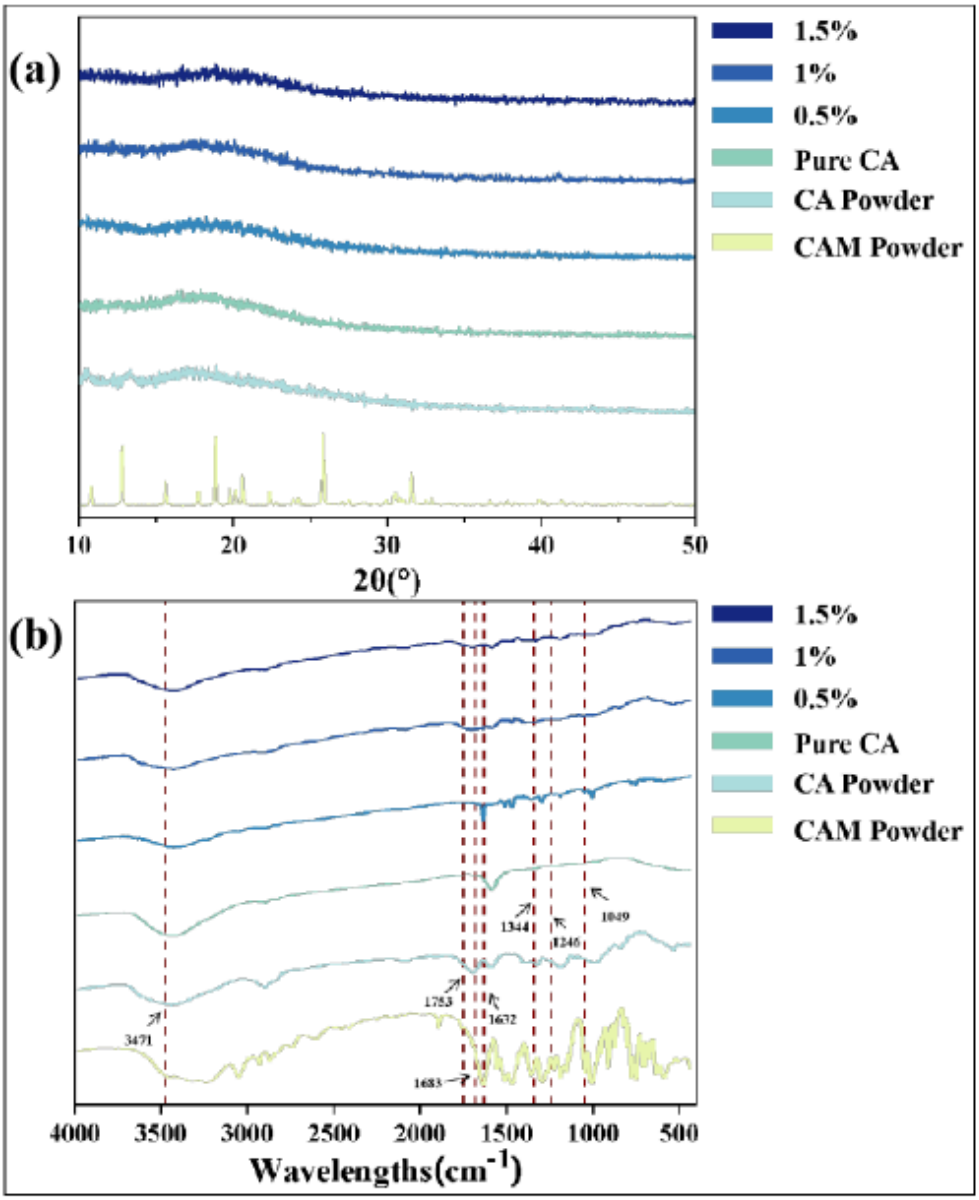

Fig. 3. (a) XRD patterns of CAM; CA; Loaded 0-1.5% CAM CA patches ;(b) FTIR spectroscopy of CAM; CA; Loaded 0-1.5% CAM CA patches.

3.3. Hydrophilicity and swelling degree of contact-lens like CA patches

Water contact angle was used to investigate the hydrophilicity of CAM-loaded contact-lens like CA patches[40]. Favorable hydrophilicity is beneficial to wound recovery[41]. Fig. 4a shows the water contact angle of CA patches loading different concentration of CAM. The contact angle of pure CA patches, CA patches loading with 0.5% CAM, 1% CAM, and 1.5% CAM were 57.3±1.5°, 57.9±2.3°, 63.2±1.7°, and 65.6±1.3°, separately.

It could be observed that improving the concentration of CAM would slightly increase the value of water contact angle for CA patches due to the reason that the addition of CAM for CA patches caused the high roughness which was corresponding to the AFM results (Fig. 2c and 2d). However, all the contact-lens like CA patches loading with various CAM maintained the water contact angle at 60°, indicating that the CA patches had good hydrophilicity, which is beneficial to treat corneal abrasions.

The swelling degree is also a crucial factor in determining the potency of fibrous scaffolds for wound healing utilizations. The swelling ratio could influence the loading and release behavior, as well as induce a moist micro-environment that provokes the wound healing process[28] . As shown in Fig. 4b, the CA patches loading with different concentrations of CAM all showed good swelling rates. After three hours, the swelling rate of pure CA patches was the highest reaching at 157.1 ± 7.3%, followed by the1.5% CAM-loaded CA patches of which the swelling rate was 156.1 ± 8.0%. While the swelling rate of 0.5% CAM-loaded CA patches was 155.3 ± 5.8%, and CA patches loading with 1% CAM owned the lowest swelling rate, which was 153.5.1 ± 6.5%. However, after 12 hours, there was no significant difference for the swelling rate of different samples. The swelling rare kept stable during the following 9 hours. The results demonstrate that contact-lens like CA patches with different concentrations of CAM had good water absorption for a long time. The higher swelling ratio of the patches are due to higher surface area of the micron fibers. And an important feature governing the functionality of patches is the ability to undergo adequately controlled swelling and maintain structural integrity for the desired time as per biological requirements[42].

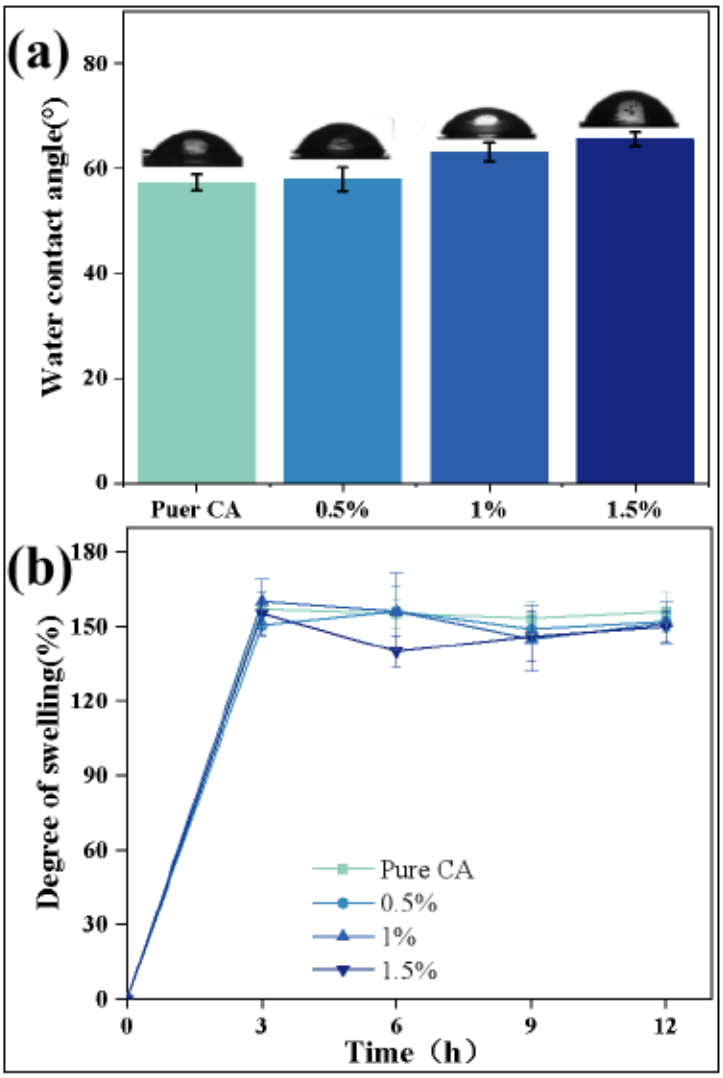

Fig. 4. (a) Water contact angle of CA patches loading different concentrations of CAM (b) Degree of swelling (%) for CA patches loading different concentrations of CAM.

3.4. Influence of CAM concentration on drug release rate and drug loading rate

The drug release behaviors of various concentrations of CAM-loaded contact-lens like CA patches were investigated in this study. Drug loading capacity (LE) and encapsulation efficiency (EE) data are shown in Table 1. The drug loading efficiency of 0.5%, 1%, and 1.5% CAM-loaded CA patches were 5.9 ± 0.3%, 6.9 ± 0.6%, and 10.2 ± 0.7%, separately. Increasing the concentration of CAM could enhance the drug loading efficiency remarkably. And the drug release curves are shown in Fig. 5. It is shown that the trends of the three curves are same. Within the first 1 hour, CAM was

released rapidly from the CA patches, and reached 40.2 ± 9.3%, 38.9 ± 2.5%, 27.8 ± 5.5% for 0.5%, 1% and 1.5% CAM-loaded CA patches, respectively. In the following time until 100 hours, the CAM release were slow and sustainable. At 96 h, the cumulative release amount of CAM for CA patches loading 0.5%, 1% and 1.5% CAM were 91.7 ± 5.2%, 92.2 ± 1.0%, and 89.0 ± 7.5%, separately. It could be found that 0.5% CAM-loaded CA patches had the highest release rate and the CAM almost totally release after 20 hours because of the reason that it had the smallest drug loading. The results show that CAM-loaded CA patches had a high drug loading capacity and could release the CAM continuously and effectively until seven days, so that had an enormous potential for treating corneal abrasions efficiently.

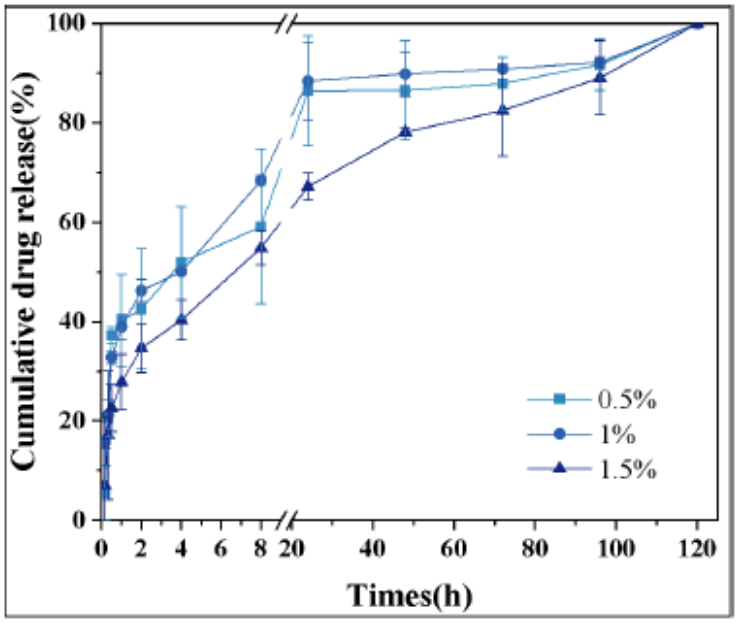

Fig. 5. Drug release rate of films loaded with different concentrations of CAM.

Table. 1

Drug loading of films loaded with different concentrations of CAM.

SAMPLE	DRUG LOADING（%）
0.5%CAM-LOADED CA PATCHES	5.90±0.34
1%CAM-LOADED CA PATCHES	6.92±0.56
1.5%CAM-LOADED CA PATCHES	10.20±0.73

Drug release data for CAM-loaded CA patches were fitted to Korsmeyer-Peppas and Higuchi models. The results were shown in Table 2. For, Regression coefficients and n

values of Korsmeyer-Peppas model were calculated. For CA patches loading 0.5%, 1% and 1.5% CAM, n values were 0.0043, 0.0039, and 0.0036, respectively. It has been reported that $n < 0.45$, Fickian diffusion is most likely[43]. While, $n < 0.45$ was established for all samples, Fickian diffusion dominates the drug release process. For Higuchi model, if the cumulative drug release content is linearly dependent on square root of time, drug release is likely to be diffusion-controlled[44]. The high R^2 values of the samples suggests that drug release from all complicated constructs is via diffusion mechanism[44].

Table. 2

Application of Korsmeyer-Peppas and Higuchi models to drug released from CA patches loading 0.5%, 1%, 1.5% CAM.

Samples	*Model*	*Equation*	*n*	R^2
0.5%CAM	Korsmeyer-Pappas	$\log (M_t/M_\infty \times 100) = 0.5976 + 0.0043 \times \log (t)$	0.0043	0.9342
	Higuchi	$M_t/M_\infty \times 100 = 2.7841 + 1.4364 \times t^{1/2}$	—	0.935
1%CAM	Korsmeyer-Pappas	$\log (M_t/M_\infty \times 100) = 0.66.3 + 0.0039 \times \log (t)$	0.0039	0.9623
	Higuchi	$M_t/M_\infty \times 100 = 0.9414 + 0.3353 \times t^{1/2}$	—	0.9646
1.5%CAM	Korsmeyer-Pappas	$\log (M_t/M_\infty \times 100) = 0.6912 + 0.0036 \times \log (t)$	0.0036	0.9534
	Higuchi	$M_t/M_\infty \times 100 = 3.4733 + 0.6408 \times t^{1/2}$	—	0.9744

3.5. CCK-8 cell viability test and L929 cell morphology study

An ideal environment for cell attachment and proliferation is critical for materials used in corneal restoration. The results of CCK-8 testing indicated that CAM-loaded CA patches show good biocompatibility. The CCK-8 assay data of L929 cells (Fig. 6) shows that the cell viability of pure CA patches and 0.5%, 1%, and 1.5% CAM-loaded CA patches in 3 days were 101.9 ± 3.2%, 101.4 ± 0.6%, 105.2 ± 4.9%, and 100.6 ± 0.3%. While after 5 days, the cell viability of CA patches and 0.5%, 1%, and 1.5% CAM-loaded CA patches were 100.6±0.4, 102.4±2.5, 102.8±2.6, and 101.8±3.6. The cell viability of each group is not much different between 5 and 3 days. The same result was also shown in the OD value, indicating that the cells have good viability, and the well have been completely covered in three days.

A principal factor to investigate material biocompatibility is cell morphology. Fluorescent images of L929 cells cultured on various CAM-loaded CA patches for 3 and 5 days are presented in Fig. 7. L929 cells cultured for 3 days showed a less sparse distribution of cells than 5 days. After 3 days of culture, it can be observed that the cells in the CAM-added sample group exhibited spindle morphology and cell density similar to those in the control group (Fig. 7a-e). When cultivated for 5 days, the cell density of each group increased significantly (Fig. 7a1-e1). In addition, as the concentration of CAM increases, the cells showed a more average distribution, and the cell morphology were 3D in CA patches rather than 2D in TCPs, which indicated that CAM has a certain role in promoting cell migration[45].

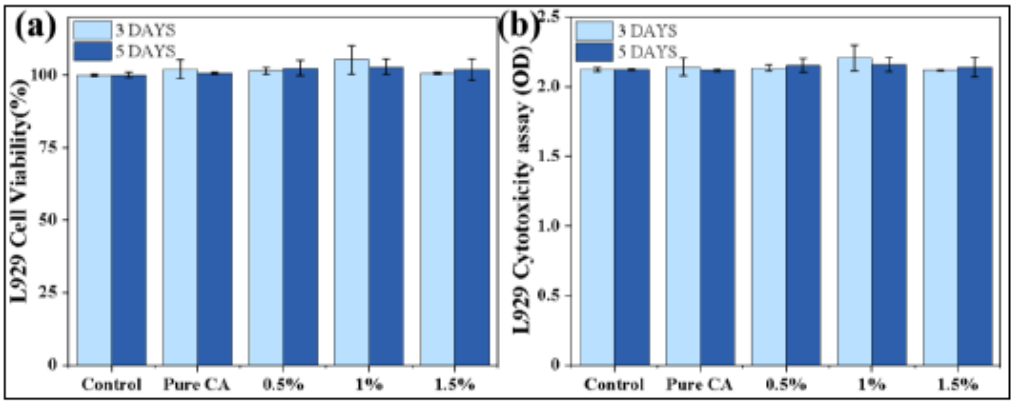

Fig. 6. (a) L929 cell viability of patches with different concentrations of CAM
(b) L929 cell OD value of patches with different concentrations of CAM.

3.6. L929 cell migration assay

The effect of CAM concentration on L929 cell migration was investigated. Figure 8 respectively shows cell migration in L929 cell monolayers in control groups, CA patches, 0.5% CAM-loaded CA patches, 1% CAM-loaded CA patches, 1.5% CAM-loaded CA patches after 0, 24, 48, and 72 hours of incubation. Migration rate was measured by ImageJ software as shown in Figure 9. After the initial 24 h incubation, the monolayers were distributed regularly (Fig. 8a1-e1). This result suggests that cells migration is not evident within the first 24 hours. At 48 hours, except for the control group, each group's monolayer appeared irregular (Fig. 8a2-e2). It indicated that patches had promoted cell to migrate. The blank area of the sample-added group is

significantly reduced (Fig. 8a3-e3) after 72 h of incubation, where 1% CAM-loaded CA patches showed the most obvious cell migration (Fig. 9), suggesting that a moderate quantity of CAM in CA patches is sufficient to enhance cell migration. Cell migration tests show that CAM-loaded CA patches have enormous potential to promote corneal restoration.

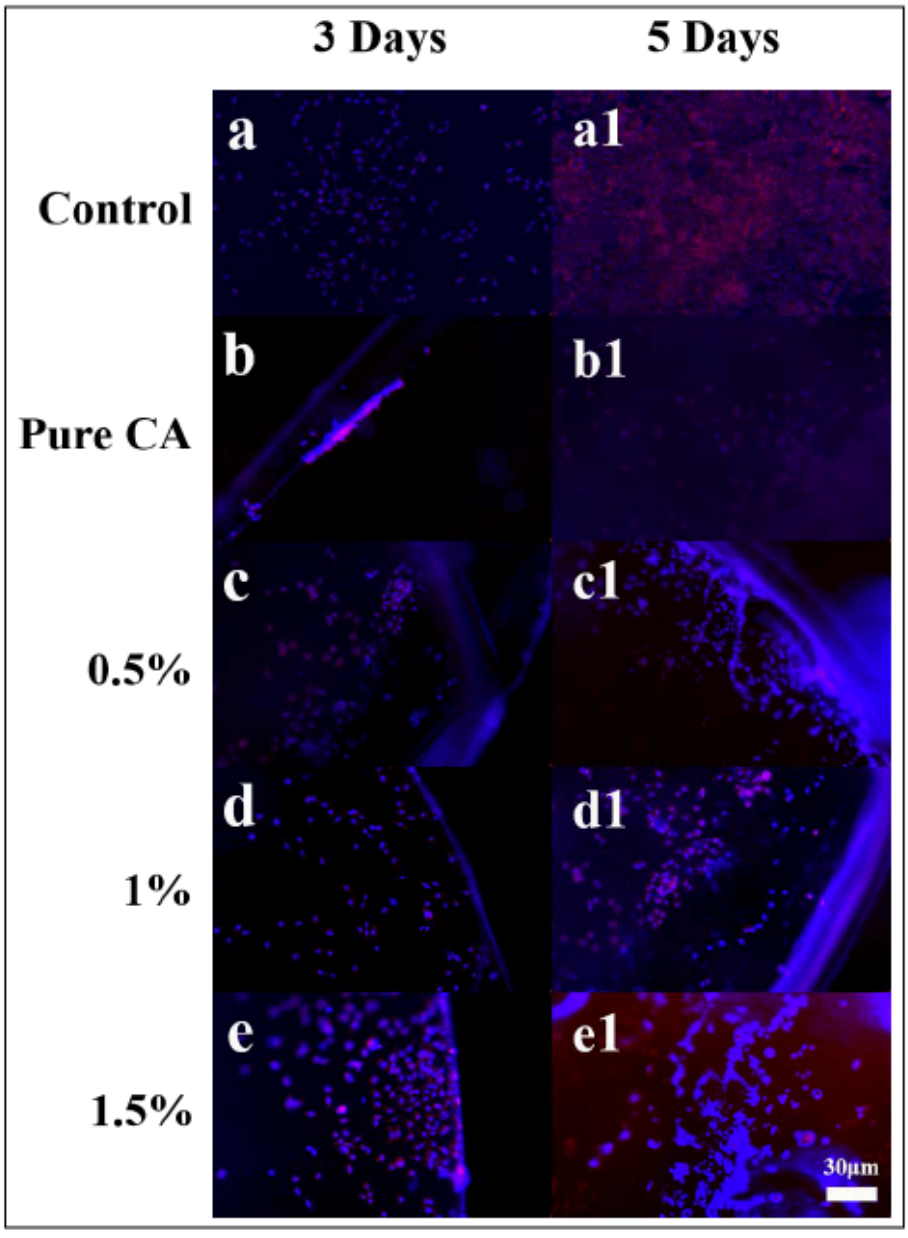

Fig. 7. Fluorescence micrographs of L929 cells grown on (a) the absence (control), (b) CA patches, and (c) 0.5% CAM-loaded CA patches, (d) 1% CAM-loaded CA patches, (e) 1.5% CAM-loaded CA patches.

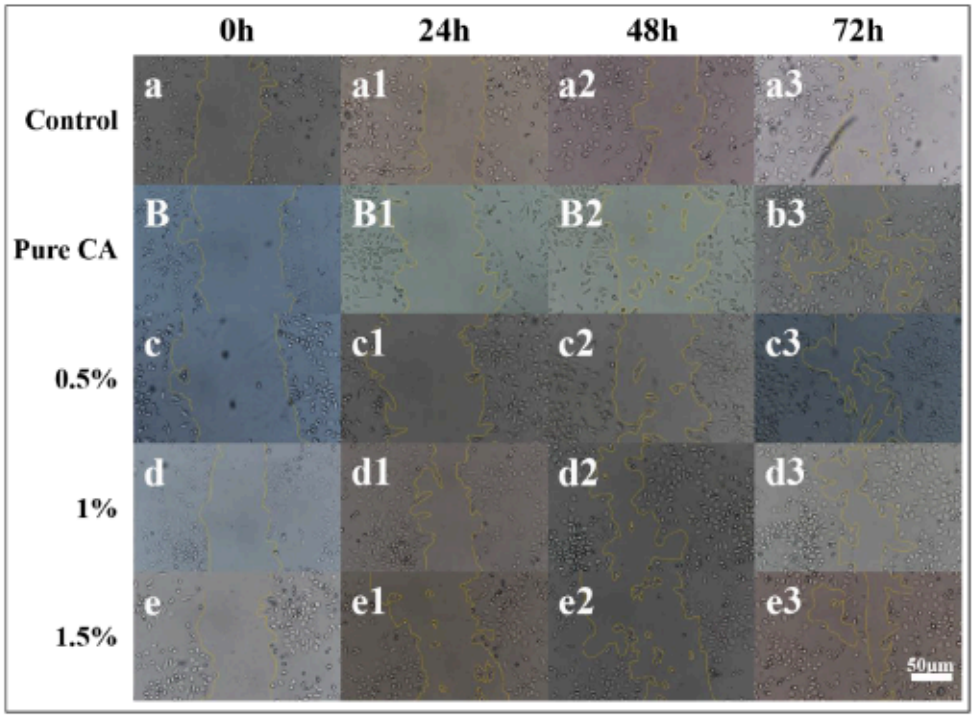

Fig. 8. Micrographs of L929 cells migrating into a scratch area over a 72h period in (a) the absence (control), (b) CA patches, and (c) 0.5% CAM-loaded CA patches, (d) 1% CAM-loaded CA patches, (e) 1.5% CAM-loaded CA patches.

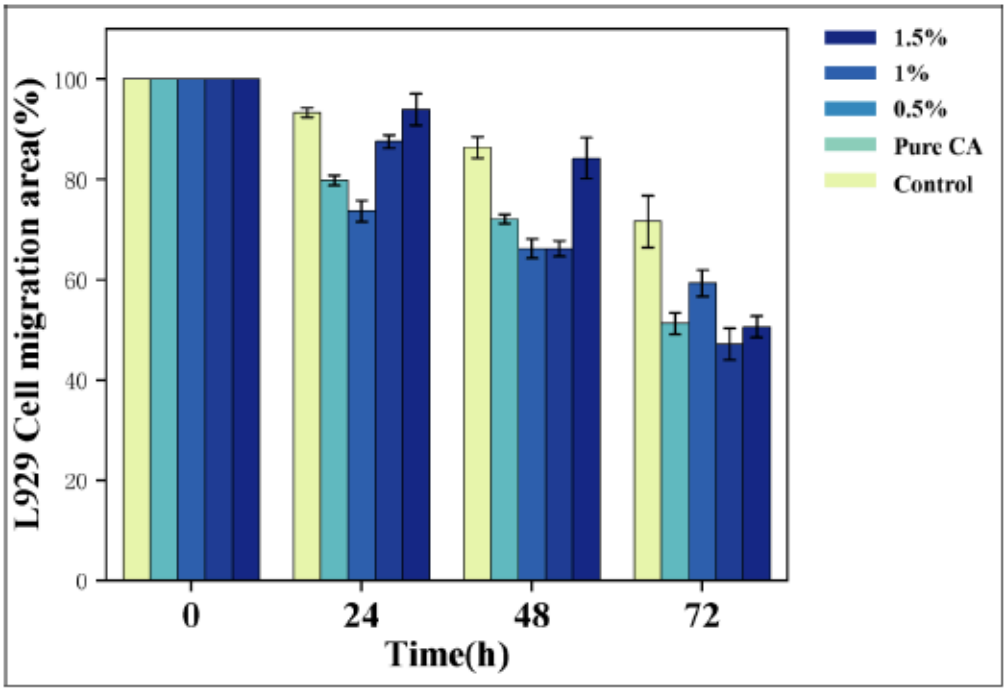

Fig. 9. L929 cell migration rate of patches with different concentrations of CAM.

4 Conclusion

In this study, the contact lens-like CAM-loaded patches were prepared via EHD printing technology. The patches had a shape like contact lens as well as good light transmittance and was suitable to be wore in eyes for corneal abrasions treatment. The results showed that the patches had the advantages of a controllable drug delivery rate and high loading efficiency. L929 cells still have high cell viability after being cultured on patches loading different concentrations of CAM, and the patches can enhance the cell migration rate, indicating that it had good biocompatibility and could promote corneal trauma repair. Compared with traditional treatment methods, the film could provide sustained and stable release of drugs and had great potential to be applied in the clinic treatment for patients suffering from corneal abrasions.

Declaration of Competing Interest

The authors declare that they have no known competing financial interests or personal relationships that could have appeared to influence the work reported in this paper.

Acknowledgements

This research was financially supported by the Natural Science Foundation of Hebei Province of China under Grant No.H2020202002.

Reference

[1] R. Channa, S.N. Zafar, J.K. Canner, R.S. Haring, E.B. Schneider, D.S. Friedman,Epidemiology of Eye-Related Emergency Department Visits, JAMA Ophthalmol, 134 (2016) 312-319, https://doi.org/10.1001/jamaophthalmol.2015.5778.

[2] Zhu, Qiang, Cheng, Hongbo, Huo, Yingnan, Mao, S.J.I.J.o. Pharmaceutics,Sustained ophthalmic delivery of highly soluble drug using pH-triggered inner layer-embedded contact lens, Int. J. Pharm., 544 (2018) 100-111, https://doi.org/10.1016/j.ijpharm.2018.04.004.

[3] C.C. Li, A.J.I. Chauhan, E.C. Research,Modeling Ophthalmic Drug Delivery by Soaked Contact Lenses, Ind. Eng. Chem. Res., 45 (2006) 3718-3734, https://doi.org/10.1021/ie0507934.

[4] B. Arias-Peso, H. Rendón-Fernández, M.A.J.V.J.o.E. Medicine,Corneal abrasion secundary to accidental trauma with face mask, Vis. J. Emerg. Med., 22 (2021), https://doi.org/10.1016/j.visj.2020.100953.

[5] C. Li, A.J.J.o.D.D.S. Chauhan, Technology,Ocular transport model for ophthalmic delivery of timolol

through p-HEMA contact lenses, J Drug Deliv Sci Technol, 17 (2007) 69-79, https://doi.org/10.1016/S1773-2247(07)50010-9.
[6] R.D. Bachu, P. Chowdhury, Z.H.F. Al-Saedi, P.K. Karla, S.H.S. Boddu,Ocular Drug Delivery Barriers-Role of Nanocarriers in the Treatment of Anterior Segment Ocular Diseases, Pharmaceutics, 10 (2018), https://doi.org/10.3390/pharmaceutics10010028.
[7] Y.M. Wu, Y.Y. Liu, X.Y. Li, D. Kebebe, B. Zhang, J. Ren, J. Lu, J.W. Li, S.Y. Du, Z.D. Liu,Research progress of in-situ gelling ophthalmic drug delivery system, Asian J. Pharm., 14 (2019) 1-15, https://doi.org/10.1016/j.ajps.2018.04.008.
[8] H.J. Jung, M. Abou-Jaoude, B.E. Carbia, C. Plummer, A.J.J.o.C.R.O.J.o.t.C.R.S. Chauhan,Glaucoma therapy by extended release of timolol from nanoparticle loaded silicone-hydrogel contact lenses, J Control Release, 165 (2013) 82-89, https://doi.org/10.1016/j.jconrel.2012.10.010.
[9] L.C. Bengani, K.H. Hsu, S. Gause, A.J.E.O.D.D. Chauhan,Contact lenses as a platform for ocular drug delivery, Expert Opin Drug Deliv, 10 (2013) 1483-1496, https://doi.org/10.1517/17425247.2013.821462.
[10] L.J. Luo, D.D. Nguyen, C.C. Huang, J.Y. Lai,Therapeutic hydrogel sheets programmed with multistage drug delivery for effective treatment of corneal abrasion, Chem. Eng. J., 429 (2022) 13, https://doi.org/10.1016/j.cej.2021.132409.
[11] I.M. Carvalho, C.S. Marques, R.S. Oliveira, P.B. Coelho, P.C. Costa, D.C.J.J.o.C.R. Ferreira,Sustained drug release by contact lenses for glaucoma treatment—A review, J Control Release, 202 (2015) 76-82, https://doi.org/10.1016/j.jconrel.2015.01.023.
[12] C. González-Chomón, A. Concheiro, C.J.T.D. Alvarez-Lorenzo,Soft contact lenses for controlled ocular delivery: 50 years in the making, Ther Deliv, 4 (2013) 1141-1161, https://doi.org/10.4155/tde.13.81.
[13] B. Wang, S. Wu, Z. Ahmad, J.-s. Li, M.-W. Chang,Co-printing of vertical axis aligned micron-scaled filaments via simultaneous dual needle electrohydrodynamic printing, European Polymer Journal, 104 (2018) 81-89, 10.1016/j.eurpolymj.2018.05.005.
[14] M. Goldberg, R. Langer, X.J.J.o.B.S. Jia,Nanostructured materials for applications in drug delivery and tissue engineering, J Biomater Sci Polym Ed, 18 (2007) 241-268, https://doi.org/10.1163/156856207779996931.
[15] M. Rahmati, D.K. Mills, A.M. Urbanska, M.R. Saeb, J.R. Venugopal, S. Ramakrishna, M. Mozafari,Electrospinning for tissue engineering applications, Prog. Mater. Sci., 117 (2021), https://doi.org/10.1016/j.pmatsci.2020.100721.
[16] S. Agarwal, A. Greiner, J.H. Wendorff,Functional materials by electrospinning of polymers, Prog. Polym. Sci., 38 (2013) 963-991, https://doi.org/10.1016/j.progpolymsci.2013.02.001.
[17] A. Moreira, D. Lawson, L. Onyekuru, K. Dziemidowicz, U. Angkawinitwong, P.F. Costa, N. Radacsi, G.R. Williams,Protein encapsulation by electrospinning and electrospraying, J Control Release, 329 (2021) 1172-1197, https://doi.org/10.1016/j.jconrel.2020.10.046.
[18] E.A. Tawfik, D.Q.M. Craig, S.A. Barker,Dual drug-loaded coaxial nanofibers for the treatment of corneal abrasion, International Journal of Pharmaceutics, 581 (2020), 10.1016/j.ijpharm.2020.119296.
[19] J.U. Park, J.H. Lee, U. Paik, Y. Lu, J.A.J.N.L. Rogers,Nanoscale patterns of oligonucleotides formed by electrohydrodynamic jet printing with applications in biosensing and nanomaterials assembly, Nano Lett., 8 (2008) 4210-4216, https://doi.org/10.1021/nl801832v.
[20] S. Wu, J.-S. Li, J. Mai, M.-W. Chang,Three-Dimensional Electrohydrodynamic Printing and Spinning of Flexible Composite Structures for Oral Multidrug Forms, Acs Applied Materials & Interfaces, 10

(2018) 24876-24885, 10.1021/acsami.8b08880.
[21] R. Konwarh, N. Karak, M.J.B.A. Misra,Electrospun cellulose acetate nanofibers: The present status and gamut of biotechnological applications, Biotechnol. Adv., 31 (2013) 421-437, https://doi.org/10.1016/j.biotechadv.2013.01.002.
[22] S. Liu, L. Tan, W. Hu, X. Li, Y.J.M.L. Chen,Cellulose acetate nanofibers with photochromic property: Fabrication and characterization, Mater. Lett., 64 (2010) 2427-2430, https://doi.org/10.1016/j.matlet.2010.08.018.
[23] A. Danion, C.J. Doillon, C.J. Giasson, S.J.O. Djouahra, v. science,Biocompatibility and Light Transmission of Liposomal Lenses, Optom Vis Sci, 84 (2007) 954-961, https://doi.org/10.1097/OPX.0b013e318157a6d5.
[24] M. Afzal, A.K. Vijay, F. Stapleton, M.D.P. Willcox,Susceptibility of Ocular Staphylococcus aureus to Antibiotics and Multipurpose Disinfecting Solutions, Antibiotics-Basel, 10 (2021), https://doi.org/10.3390/antibiotics10101203.
[25] T.T.V. Tong, T.T. Cao, N.H. Tran, T.K.V. Le, D.C. Le,Green, Cost-Effective Simultaneous Assay of Chloramphenicol, Methylparaben, and Propylparaben in Eye-Drops by Capillary Zone Electrophoresis, J. Anal. Methods Chem., 2021 (2021) 11, https://doi.org/10.1155/2021/5575701.
[26] Y. Wei, Y. Hu, X. Shen, X. Zhang, S.J.E.J.o.P. Mao, Biopharmaceutics,Design of circular-ring film embedded contact lens for improved compatibility and sustained ocular drug delivery, Eur J Pharm Biopharm, 157 (2020) 28-37, https://doi.org/10.1016/j.ejpb.2020.09.010.
[27] B. Wang, M. Wang, M.W. Chang, Z. Ahmad, J. Huang, J.S.J.M.L. Li,Non-concentric multi-compartment fibers fabricated using a modified nozzle in single-step electrospinning, Mater. Lett., 202 (2017) 134-137, https://doi.org/10.1016/j.matlet.2017.05.035.
[28] A.A. Aly, M.K.J.I.J.o.P. Ahmed,Nanofibers of cellulose acetate containing ZnO nanoparticles/graphene oxide for wound healing applications, Int. J. Pharm., 598 (2021), https://doi.org/10.1016/j.ijpharm.2021.120325.
[29] A. Nu, A. Hl, B. Sh, C. Shl, A.J.A.S.S. Hp,Surface functionalization of dual growth factor on hydroxyapatite-coated nanofibers for bone tissue engineering, Appl. Surf. Sci., 520, https://doi.org/10.1016/j.apsusc.2020.146311.
[30] Y. Zhao, S. Yu, X. Wu, H. Dai, W. Liu, R. Tu, T. Goto,Construction of macroporous magnesium phosphate-based bone cement with sustained drug release, Materials & Design, 200 (2021), https://doi.org/10.1016/j.matdes.2021.109466.
[31] B. Wang, Z. Ahmad, J. Huang, J.S. Li, M.W.J.C.E.J. Chang,Development of Random and Ordered Composite Fiber Hybrid Technologies for Controlled Release Functions, Chem. Eng. J., 343 (2018) 379-389, https://doi.org/10.1016/j.cej.2018.03.021.
[32] M.A. Zarandi, P. Zahedi, I. Rezaeian, A. Salehpour, M. Gholami, B.J.N.I. Motealleh,Drug release, cell adhesion and wound healing evaluations of electrospun carboxymethyl chitosan/polyethylene oxide nanofibres containing phenytoin sodium and vitamin C, IET Nanobiotechnol, 9 (2015) 191-200, https://doi.org/10.1049/iet-nbt.2014.0030.
[33] J. Siepmann, N.A.J.I.J.o.P. Peppas,Higuchi equation: Derivation, applications, use and misuse, Int. J. Pharm., 418 (2011) 6-12, https://doi.org/10.1016/j.ijpharm.2011.03.051.
[34] A.A. Menazea, M.K.J.J.o.M.S. Ahmed,Wound healing activity of Chitosan/Polyvinyl Alcohol embedded by gold nanoparticles prepared by nanosecond laser ablation, J. Mol. Struct., 1217 (2020), https://doi.org/10.1016/j.molstruc.2020.128401.
[35] S. Puttipipatkhachorn, J. Nunthanid, K. Yamamoto, G.E.J.J.o.C.R.O.J.o.t.C.R.S. Peck,Drug physical

state and drug-polymer interaction on drug release from chitosan matrix films, J Control Release, 75 (2001) 143-153, https://doi.org/10.1016/S0168-3659(01)00389-3.
[36] J. Liu, Y. Xiao, C.J.J.o.P.S. Allen,Polymer–drug compatibility: A guide to the development of delivery systems for the anticancer agent, ellipticine, J Pharm Sci, 93 (2004) 132-143, https://doi.org/10.1002/jps.10533.
[37] F. Topuz, M.E. Kilic, E. Durgun, G. Szekely,Fast-dissolving antibacterial nanofibers of cyclodextrin/antibiotic inclusion complexes for oral drug delivery, J. Colloid Interface Sci., 585 (2021) 184-194, https://doi.org/10.1016/j.jcis.2020.11.072.
[38] M.S. Kamath, S.S.S.J. Ahmed, M. Dhanasekaran, S.W. Santosh,Polycaprolactone scaffold engineered for sustained release of resveratrol: therapeutic enhancement in bone tissue engineering, Int. J. Nanomedicine, 9 (2014) 183-195, https://doi.org/10.2147/ijn.S49460.
[39] M. Bayrakci, M. Keskinates, B.J.M.S. Yilmaz, E. C,Antibacterial, thermal decomposition and in vitro time release studies of chloramphenicol from novel PLA and PVA nanofiber mats, Mat. Sci. Eng C-Mater., 122 (2021), https://doi.org/0.1016/j.msec.2021.111895.
[40] B. Jańczuk, T. Biaopiotrowicz, E.J.J.o.C. Chibowski, I. Science,Interpretation of the contact angle in marble/organic liquid film-water system, Mater. Chem. Phys., 16 (1987) 489-499, https://doi.org/10.1016/0254-0584(87)90069-1.
[41] X. Ji, R. Li, W. Jia, G. Liu, Z.J.A.A.B.M. Cheng,Co-Axial Fibers with Janus-Structured Sheaths by Electrospinning Release Corn Peptides for Wound Healing, ACS Appl. Bio Mater., 3 (2020) 6430-6438, https://doi.org/10.1021/acsabm.0c00860.
[42] S. Wüst, M.E. Godla, R. Müller, S.J.A.B. Hofmann,Tunable hydrogel composite with two-step processing in combination with innovative hardware upgrade for cell-based three-dimensional bioprinting, Acta Biomater., 10 (2014) 630-640, https://doi.org/10.1016/j.actbio.2013.10.016.
[43] A. Jain, S.K.J.C. Jain, P.o. Lipids,In vitro release kinetics model fitting of liposomes: An insight, Chem. Phys. Lipids, 201 (2016) 28-40, https://doi.org/10.1016/j.chemphyslip.2016.10.005.
[44] C. Sara,Modeling and comparison of release profiles: Effect of the dissolution method, Eur J Pharm Sci, 106 (2017) 352-361, https://doi.org/10.1016/j.ejps.2017.06.021.
[45] Y. Sun, X. Chi, H. Meng, M. Ma, J. Wang, Z. Feng, Q. Quan, G. Liu, Y. Wang, Y. Xie, Y. Zheng, J. Peng,Polylysine-decorated macroporous microcarriers laden with adipose-derived stem cells promote nerve regeneration in vivo, Bioact. Mater., 6 (2021) 3987-3998, https://doi.org/10.1016/j.bioactmat.2021.03.029.